Am J Physiol Renal Physiol 301: F94–F100, 2011.
First published April 20, 2011; doi:10.1152/ajprenal.00650.2010.

Tumor necrosis factor-α is an endogenous inhibitor of Na^+-K^+-$2Cl^-$ cotransporter (NKCC2) isoform A in the thick ascending limb

Sailaja Battula, Shoujin Hao, Paulina L. Pedraza, Charles T. Stier, and Nicholas R. Ferreri

Department of Pharmacology, New York Medical College, Valhalla, New York

Submitted 3 November 2010; accepted in final form 18 April 2011

Battula S, Hao S, Pedraza PL, Stier CT, Ferreri NR. Tumor necrosis factor-α is an endogenous inhibitor of Na^+-K^+-2Cl^- cotransporter (NKCC2) isoform A in the thick ascending limb. *Am J Physiol Renal Physiol* 301: F94–F100, 2011. First published April 20, 2011; doi:10.1152/ajprenal.00650.2010.—The effects of TNF gene deletion on renal Na^+-K^+-$2Cl^-$ cotransporter (NKCC2) expression and activity were determined. Outer medulla from $TNF^{-/-}$ mice exhibited a twofold increase in total NKCC2 protein expression compared with wild-type (WT) mice. This increase was not observed in $TNF^{-/-}$ mice treated with recombinant human TNF (hTNF) for 7 days. Administration of hTNF had no effect on total NKCC2 expression in WT mice. A fourfold increase in NKCC2A mRNA accumulation was observed in outer medulla from $TNF^{-/-}$ compared with WT mice; NKCC2F and NKCC2B mRNA accumulation was similar between genotypes. The increase in NKCC2A mRNA accumulation was attenuated when $TNF^{-/-}$ mice were treated with hTNF. Bumetanide-sensitive O_2 consumption, an in vitro correlate of NKCC2 activity, was 2.8 ± 0.2 nmol·min^{-1}·mg^{-1} in medullary thick ascending limb tubules from WT, representing ~40% of total O_2 consumption, whereas, in medullary thick ascending limb tubules from $TNF^{-/-}$ mice, it was 5.6 ± 0.3 nmol·min^{-1}·mg^{-1}, representing ~60% of total O_2 consumption. Administration of hTNF to $TNF^{-/-}$ mice restored the bumetanide-sensitive component to ~30% of total O_2 consumption. Ambient urine osmolality was higher in $TNF^{-/-}$ compared with WT mice (2,072 ± 104 vs. 1,696 ± 153 mosmol/kgH_2O, $P < 0.05$). The diluting ability of the kidney, assessed by measuring urine osmolality before and after 1 h of water loading also was greater in $TNF^{-/-}$ compared with WT mice (174 ± 38 and 465 ± 81 mosmol/kgH_2O, respectively, $P < 0.01$). Collectively, these findings suggest that TNF plays a role as an endogenous inhibitor of NKCC2 expression and function.

Na^+-K^+-$2Cl^-$ cotransporter isoforms; medullary thick ascending limb; tumor necrosis factor; Na^+-K^+-$2Cl^-$ cotransporter A; kidney

THE THICK ASCENDING LIMB (TAL) is water impermeable and responsible for reabsorption of ~25% of the filtered load of sodium by the kidney. These features facilitate the maintenance of the high medullary interstitial osmolality, essential for conservation of the renal countercurrent exchange system and ability of the kidney to produce concentrated or dilute urine. These essential renal mechanisms are accomplished by coordinated ion transport pathways in the TAL, including the bumetanide/furosemide-sensitive apical Na^+-K^+-$2Cl^-$ cotransporter (NKCC2), renal outer medullary potassium channels, Na^+/H^+ exchanger, Na^+-K^+-ATPase, and chloride channels. Three NKCC2 variants (NKCC2A, NKCC2F, NKCC2B) are derived from the NKCC2 gene, *Slc12a1*, by differential splicing of exon 4, which encodes part of transmembrane 2 (TM2) and intracellular loop connecting TM2 and TM3 (33). Because these isoforms differ in their distribution along the nephron and in their capacity and affinity for ion transport, understanding the regulation of these isoforms is of interest.

Cytokines such as TNF and IL-1 affect ion transport mechanism in epithelial cells by regulating both expression and activity of transport proteins. For instance, IL-1 injected intravenously causes natriuresis (4) and inhibits Na^+-K^+-ATPase in the inner medullary collecting duct (49). TNF exerts direct inhibitory effects on the expression and epithelial sodium channel activity (1a). Acute renal failure (ARF) is mediated, in part, by TNF (7) and is associated with decreases in major transporters (23, 38). The defect in urine concentrating ability in conditions such as sepsis is associated with TNF-mediated downregulation of NKCC2 and other ion transporters in the kidney (38). TNF also causes downregulation of NKCC1 in the renal cortex and inner medulla (22). No information is available regarding the role of cytokines and, in particular TNF, on the regulation of NKCC2 isoforms.

Our laboratory previously has explored mechanisms of TNF production and function in the medullary TAL (mTAL). For instance, TNF production is induced by lipopolysaccharide, angiotensin II, and activation of the calcium-sensing receptor in cultured mTAL cells (10, 13, 26, 48). Moreover, endogenous, as well as exogenous, TNF inhibits ^{86}Rb uptake in mTAL cells and is natriuretic in vivo (10, 39). Our laboratory recently determined that inhibition of apical chloride uptake in response to calcium-sensing receptor activation in primary cultured mTAL cells is nuclear factor of activated T cell 5 dependent (16). As nuclear factor of activated T cell 5 activation increases TNF production in mTAL cells (17), and since chloride uptake in this nephron segment occurs mainly via NKCC2, we tested the hypothesis that TNF acts as an endogenous inhibitor of NKCC2 in vivo.

MATERIALS AND METHODS

Chemicals and reagents. The NKCC2 antibody was purchased from Chemicon and used at 1:3,000 dilution for immunoblot analysis. Collagenase (type 1A) was obtained from Sigma (St. Louis, MO), recombinant human TNF (hTNF) from Invitrogen (CA), and polyvinylidene difluoride membranes were from Amersham (Arlington Heights, IL); all chemicals were of the highest grade commercially available.

Mice. Male B6129S-*Tnftm1Gkl*/J TNF-deficient mice ($TNF^{-/-}$) congenic on the C57BL/6J genetic background, and C57BL/6J [wild-type (WT)] mice were purchased from The Jackson Laboratory, maintained on a standard diet (0.6% NaCl diet, Harlan Teklad), and given tap water ad libitum. Experimental procedures were approved by, and conducted in accordance with, institutional and international guidelines for the welfare of animals (animal welfare assurance number A3362-01, Office of Laboratory Animal Welfare, PHS, National Institutes of Health). Blood was collected by cardiac puncture, at the time of death, for determination of plasma parameters. Kidneys were collected, and the outer medulla (OM) dissected and snap frozen in

Address for reprint requests and other correspondence: N. R. Ferreri, Dept. of Pharmacology, New York Medical College, Valhalla, NY 10595 (e-mail: nick_ferreri@nymc.edu).

liquid nitrogen and stored at −80°C until use. In some experiments, mice were treated for 7 days with hTNF (10 ng·g body wt^{-1}·day^{-1}) by intraperitoneal injection.

Determination of serum/urine parameters. Plasma sodium, potassium, free ionized calcium, and hematocrit were measured using a GEM Premier 3000 analyzer. Chloride, blood urea nitrogen, and creatinine were measured with an Olympus 640e Clinical Chemistry Analyzer (Antech Diagnostics). Urine osmolality was determined using a vapor-pressure osmometer (Wescor, Logan, UT; Vapro no. 5520).

Isolation of mTAL tubules. mTAL tubules (90–95% purity) were isolated from mice, as previously described (16). Briefly, mice were anesthetized with isofluorane, and the kidneys were perfused with sterile 0.9% saline via retrograde perfusion from the aorta. Kidneys were removed and then cut along the corticopapillary axis, and the OM excised, minced with a sterile blade, and incubated for 10 min at 37°C in a 0.01% collagenase solution gassed with 95% oxygen. The suspension was sedimented on ice and mixed with Hanks' balanced salt solution (HBSS) containing 2% BSA, and the supernatant containing the crude suspension of tubules was collected. The collagenase digestion was repeated three times with the remaining undigested tissue, and the combined supernatants were centrifuged for 10 min, resuspended in HBSS, and filtered through a 53-μm nylon mesh membrane (Fisher Scientific, Springfield, NJ). The filtered solution was discarded, and the tubules retained on the mesh were resuspended in HBSS, centrifuged at 500 rpm for 10 min, and resuspended in RPMI 1640 medium.

Western blotting. Tissue was placed in ice-cold sucrose isolation buffer at pH 7.6 (250 mM sucrose, 10 mM triethanolamine, and protease inhibitors: 0.1 mg/ml phenazine methyl sulfonyl fluoride and 1 μg/ml leupeptin) (8) and homogenized using a tissue homgenizer (Pro Scientific); protein concentration was measured using a Bio-Rad assay kit. Twenty micrograms of renal OM protein were used for detection of NKCC2, and an appropriate volume of 5× loading buffer was added to each sample, which was then heated at 60°C for 15 min. Proteins were separated on a 7.5% SDS-polyacrylamide gel and electrophoretically transferred to a polyvinylidene difluoride membrane. Following blocking at room temperature for 1 h with 5% skim milk, the membrane was probed overnight with anti-NKCC2 antibody, followed by incubation with horseradish peroxidase-conjugated rabbit secondary antibody (1:10,000). Membranes were washed, and proteins detected by enhanced chemiluminescence (Amersham). Blots were stripped and probed with anti-β-actin (1:40,000, Santa Cruz Biotechnology) for 20 min, followed by mouse secondary antibody (1:20,000), and the intensity of NKCC2 was normalized to that of β-actin.

Isolation of total RNA and amplification of cDNA fragments. One milliliter of TRIZOL reagent was added to the OM or renal cortex and incubated at room temperature for 10 min. Chloroform (0.2 ml) was then added at room temperature, and, after 3 min, the sample was centrifuged for 15 min at 12,000 rpm and 4°C. Isopropanol (3 vol) was added to the recovered supernatant, and the mixture was incubated at room temperature for 10 min and then centrifuged for 15 min at 12,000 rpm and 4°C. The supernatant was discarded, and the pellet washed in 1 ml of 75% ethanol, mixed gently, and centrifuged for 5 min at 7,500 rpm and 4°C. The supernatant was removed, and the pellet dried for 5–10 min. Finally, the RNA pellet was resuspended in 50 μl of RNase-free dH_2O and stored at −70°C. After total RNA was treated with deoxyribonuclease I for 30 min, a 3-μg aliquot was used for cDNA synthesis using the Superscript Preamplification system (Life Technologies) in a 20-μl reaction mixture containing Superscript II reverse transcriptase (200 U/μl) and random hexamers (50 ng/μl). The reaction was incubated at room temperature for 10 min to allow extension of the primers by reverse transcriptase, then at 42°C for 50 min, 70°C for 15 min, and 4°C for 5 min. The cDNA fragments were separated on a 1% agarose gel and stained with ethidium bromide.

Assessment of target gene expression. A 0.5-μg aliquot of total RNA was converted to cDNA using random primers and PowerScript RT (Clontech), according to the manufacturer's protocol. The cDNA from each RNA sample was placed in a 20-μl RT-PCR mixture using the FastStart DNA Master SYBR Green I kit (Roche), supplemented with 3 mM $MgCl_2$ and Platinum Taq polymerase (Invitrogen). Quantitative real-time PCR (qRT-PCR) was used to determine accumulation of mRNA for NKCC2 isoforms. The specific primer pairs for murine NKCC2A, B, and F isoforms used in this study were designed based on accession no. NM_183354, NM_001079690, and U20974.1, respectively (NKCC2A: forward 5′-GGTAACCTCTATCACTGGGT-3′, reverse 5′-GTCATTGGTTGGATCCACCA-3′; NKCC2F: forward 5′-GTCATCATCATTGGCCTG-3′, reverse 5′-GAATCCCACCACATACATAG-3′; and NKCC2B: forward 5′-GCCGTGACAGTGACAGCCAT-3′, reverse 5′-GGATCCACCATCATTGAATCG-3′). Input cDNAs were normalized using the housekeeping gene, β-actin, and the efficiency of primer pair amplification was determined using a standard curve (32, 34). Relative NKCC2 isoform mRNA accumulation was calculated using the $2(-\Delta\Delta CT)$ method (24).

Measurement of oxygen consumption. Oxygen consumption was measured as previously described (9). Briefly, 100 μl of mTAL tubule suspension were dispensed into each well of a 96-well round bottom plate coated with a proprietary biosensor, which fluoresces when oxygen is depleted (BD Biosciences). The plates were read using a Bio-Tek FLx 800 fluorescence microplate reader, set to read the bottom of the plate with excitation/emission wavelengths at 485/620 nm; fluorescence readings were converted to oxygen consumption rates using the KC4 (Kineticalc) program, according to the manufacturer's protocol (Bio-Tek instruments). Protein concentration of the tubules was determined using a protein assay kit (Biorad). The percent inhibition in the presence of bumetanide was calculated as the difference between total oxygen consumption and oxygen consumption in tubules treated with 250 μM bumetanide, divided by the total oxygen consumption, and multiplied by 100.

Water restriction and water loading protocols. WT and $TNF^{-/-}$ mice were maintained in filter-top cages and given food and water ad libitum. Urine was collected by placing each mouse into a clean glass container with a metal wire platform until spontaneous voiding took place (25). Urine samples were transferred into 0.5 ml Eppendorf tubes, wrapped with parafilm, and placed immediately on ice to prevent evaporation. Mice were then returned to filter-top cages and deprived of drinking water for 24 h, after which time urine was collected as described above. For the water-loading protocol, the weight of each mouse was recorded, and urine collected as indicated above. Next, each mouse was given an acute water load by oral gavage, equivalent to 4% of their body weight, and placed in the filter-top cages without access to drinking water until the end of the study. One hour after the gavage, voiding was facilitated by gentle bladder massage, and urine was collected for analysis.

Statistical analysis. All data are presented as means ± SE. Multiple-group comparisons were made using one-way ANOVA, followed by a Newman-Keuls test; paired Student's *t*-tests were used as indicated. A P value < 0.05 was considered statistically significant.

RESULTS

Clinical chemistry analysis of WT and $TNF^{-/-}$ mice. Plasma electrolyte concentration, as well as hydration status, and indicators of renal function were compared in WT and $TNF^{-/-}$ mice. No significant differences in plasma parameters, including Na^+, K^+, Ca^{2+}, Cl^-, blood urea nitrogen, creatinine, and hematocrit, were observed between WT and the $TNF^{-/-}$ mice (Table 1).

Elevated total NKCC2 protein in $TNF^{-/-}$ mice. NKCC2 protein expression in the OM was compared in untreated

Table 1. *Comparison of WT and TNF-deficient mice*

Parameter	WT	$TNF^{-/-}$
Sodium, mmol/l	147.6 ± 0.6	147.6 ± 0.7
Potassium, mmol/l	5.4 ± 0.1	5.4 ± 0.1
Chloride, mmol/l	114.5 ± 0.2	114.0 ± 0.3
Calcium, mmol/l	1.07 ± 0.03	1.01 ± 0.03
Hematocrit, %	43.9 ± 0.9	44.9 ± 0.3
BUN, mg/dl	33.5 ± 1.1	31.1 ± 1.7
Creatinine, mg/dl	0.25 ± 0.02	0.20 ± 0.01

Values are means ± SE. WT, wild type; BUN, blood urea nitrogen.

age-matched WT and $TNF^{-/-}$ mice, as ~80% of renal structures in the OM are TAL tubules. Western blot analysis indicated there was approximately a twofold increase in NKCC2 expression in the OM obtained from $TNF^{-/-}$ mice compared with the expression in WT mice (Fig. 1). As selective activation of the 55-kDa TNF receptor 1 (TNFR1), by administration of hTNF, induces natriuresis in mice (39), the ability of 10 ng hTNF·g body wt^{-1}·day^{-1} to suppress NKCC2 levels was evaluated in $TNF^{-/-}$ mice. This dose of TNF did not induce signs of inflammation in a previous study (40). Indeed, the increase in NKCC2 protein expression in $TNF^{-/-}$ mice was completely reversed in the OM of $TNF^{-/-}$ mice treated with hTNF (Fig. 1*A*). In contrast, administration of hTNF to WT mice did not alter total NKCC2 protein expression (Fig. 1*B*).

TNF regulates NKCC2A isoform mRNA accumulation. Our laboratory recently demonstrated that NKCC2 isoforms A and F are present in mouse mTAL tubules and primary cultured mTAL cells (16). Accordingly, NKCC2 isoform mRNA accumulation was measured in the OM of WT, $TNF^{-/-}$, and $TNF^{-/-}$ mice treated with hTNF to determine whether genetic deletion of TNF, or repletion in $TNF^{-/-}$ mice, influences NKCC2 isoform expression and evaluate whether the increase in NKCC2 protein expression is a function of increased mRNA accumulation. Analysis by qRT-PCR revealed an approximate fourfold increase in NKCC2A mRNA accumulation in the OM from $TNF^{-/-}$ compared with WT mice that was markedly attenuated when $TNF^{-/-}$ mice were treated with hTNF (2.0 ± 0.2 vs. 1.1 ± 0.1; Fig. 2*A*). Neither NKCC2F mRNA accumulation in the OM nor NKCC2B mRNA accumulation in renal cortex was affected by TNF gene deletion or treatment with hTNF, suggesting that compensatory changes in these isoforms are not evident in $TNF^{-/-}$ mice (Fig. 2, *B* and *C*). As only the TAL segment of the nephron (including the macula densa in the cortex) expresses NKCC2, the data suggest a selective effect of TNF gene deletion on NKCC2A expression in the TAL.

NKCC2 activity in WT and $TNF^{-/-}$ mice. As a large component of O_2 consumption (~50–60%) in the TAL is committed to Na^+ transport, determination of O_2 consumption is useful for evaluating alterations in ion transport mechanisms (5, 47). Bumetanide-sensitive O_2 consumption, an in vitro correlate of NKCC2 activity, was evaluated in freshly isolated mTAL tubules obtained from WT, $TNF^{-/-}$, and $TNF^{-/-}$ mice treated with hTNF, to determine whether the increases in NKCC2A mRNA accumulation and total NKCC2 protein expression in $TNF^{-/-}$ mice were associated with an increase in NKCC2 activity. Total O_2 consumption was elevated in mTAL tubules from $TNF^{-/-}$ compared with WT mice, an effect that was negated by treatment of $TNF^{-/-}$ mice with hTNF (Fig. 3*A*). Similarly, the elevated bumetanide-sensitive O_2 consumption observed in $TNF^{-/-}$ compared with WT mice was diminished when $TNF^{-/-}$ mice were treated with hTNF (Fig. 3*A*). A comparison of bumetanide-sensitive O_2 consumption between WT, $TNF^{-/-}$, and $TNF^{-/-}$ mice treated with hTNF is presented in Fig. 3*B*. Collectively, these data suggest a greater fraction of total O_2 consumption is devoted to the function of NKCC2 in mTAL of $TNF^{-/-}$ compared with WT mice.

Ambient urine osmolality is increased in $TNF^{-/-}$ compared with WT mice. Since we observed a specific increase of NKCC2A mRNA accumulation and bumetanide-sensitive O_2 consumption in untreated $TNF^{-/-}$ mice, we hypothesized that ambient osmolality might be elevated in these mice. Indeed, ambient urine osmolality was higher in $TNF^{-/-}$ compared with WT mice (2,072 ± 104 vs. 1,696 ± 153 mosmol/kgH_2O, Fig. 4). The concentrating ability of the kidney was then assessed by measuring urine osmolality before and after water deprivation for 24 h. The urine osmolalities attained

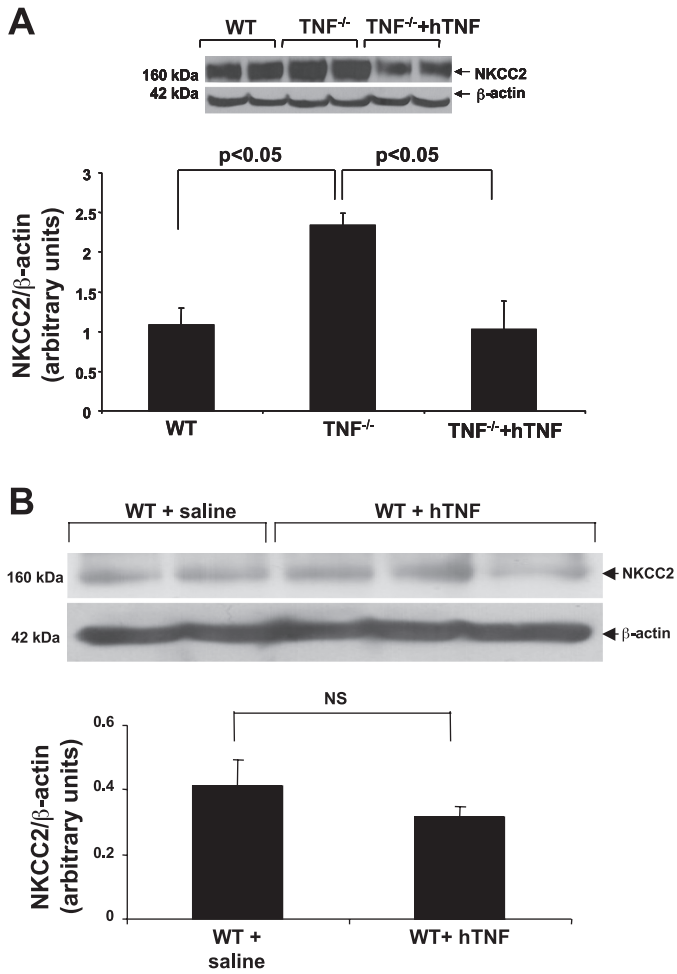

Fig. 1. Na^+-K^+-$2Cl^-$ cotransporter (NKCC2) expression is elevated in $TNF^{-/-}$ compared with wild-type (WT) mice. Total NKCC2 protein expression was analyzed by Western blot of homogenized renal outer medulla (OM) from WT, $TNF^{-/-}$, and $TNF^{-/-}$ mice treated for 7 days with human TNF (hTNF; 10 ng·g BW^{-1}·day^{-1}; *A*), and WT mice treated with saline or hTNF for 7 days (*B*). Representative blots from five similar experiments are shown in the *top* panels, and the means ± SE of NKCC2 expression normalized against β-actin expression are shown in the *bottom* panels. NS, not significant.

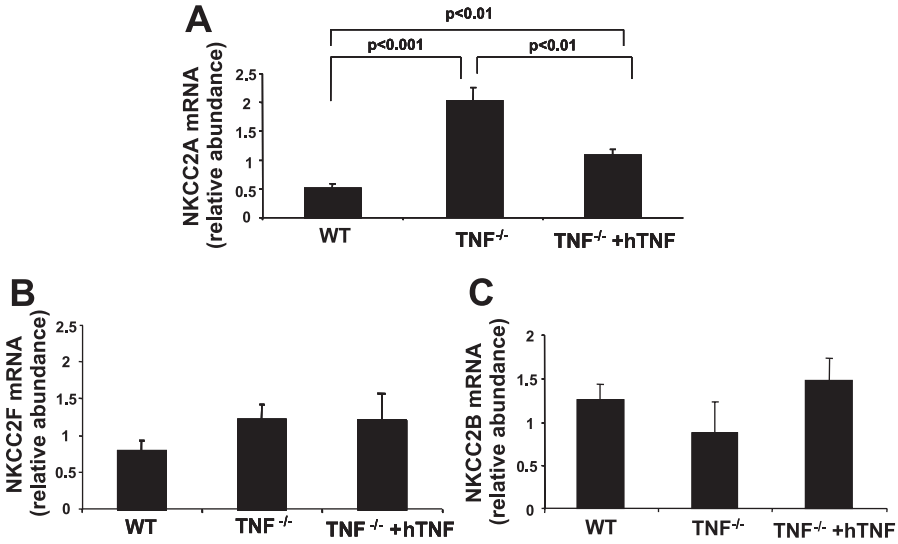

Fig. 2. Genetic deletion of TNF increases NKCC2A mRNA accumulation. Accumulation of NKCC2A (*A*) and NKCC2F (*B*) mRNA was determined by quantitative RT-PCR in OM of WT, $TNF^{-/-}$, and $TNF^{-/-}$ mice treated with hTNF, as indicated above. *C*: relative mRNA accumulation of NKCC2B in renal cortex from WT, $TNF^{-/-}$, and $TNF^{-/-}$ mice treated with hTNF. Values are means ± SE; $n = 3$–5.

after 24 h of water deprivation were similar in WT and $TNF^{-/-}$ mice (3,706 ± 43 vs. 3,625 ± 106 mosmol/kgH_2O, Fig. 4). These data suggest that increased NKCC2 activity in $TNF^{-/-}$ mice contributes to an increase in ambient osmolality, while the maximal renal concentrating effect in response to water deprivation is intact in these mice.

$TNF^{-/-}$ mice exhibit enhanced urinary diluting ability. The TAL is the major segment where the separation of water and solute occurs and, therefore, also is involved in the diluting ability of the kidney. Accordingly, urine osmolality was determined before and 1 h after WT and $TNF^{-/-}$ mice were water loaded by oral gavage to assess the diluting ability of the kidney. Urine osmolality in WT and $TNF^{-/-}$ mice 1 h after water load was 465 ± 81 and 174 ± 38 mosmol/kgH_2O, respectively ($P < 0.01$, Fig. 5), indicating that the diluting capacity of the kidney was greater in $TNF^{-/-}$ compared with WT mice.

DISCUSSION

We demonstrated that total NKCC2 protein expression in the OM and activity in freshly isolated mTAL tubules from $TNF^{-/-}$ was elevated compared with that in WT mice. The increase in NKCC2 protein expression was associated with differential regulation of NKCC2 isoforms, as qRT-PCR analysis revealed a specific increase of NKCC2A mRNA accumulation in $TNF^{-/-}$ mice, which was not accompanied by changes in either the NKCC2F or NKCC2B isoforms. Increases in NKCC2 protein expression, NKCC2A mRNA accumulation, and NKCC2 activity in $TNF^{-/-}$ mice were inhibited after treatment with hTNF (a TNFR1 agonist in mice),

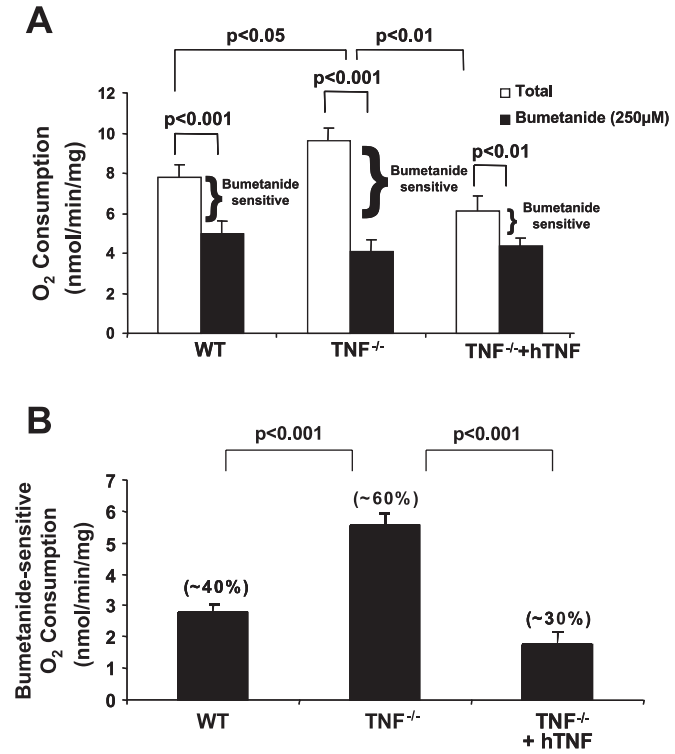

Fig. 3. Elevated levels of bumetanide-sensitive O_2 consumption in TNF-deficient mice. *A*: O_2 consumption. *B*: bumetanide-sensitive O_2 consumption. O_2 consumption was measured in freshly isolated medullary thick ascending limb (mTAL) tubules from 3 groups, WT, $TNF^{-/-}$, and $TNF^{-/-}$ mice treated with hTNF, and incubated in the presence or absence of bumetanide (250 μM) for 1 h at 37°C. Values are means ± SE; $n = 3$.

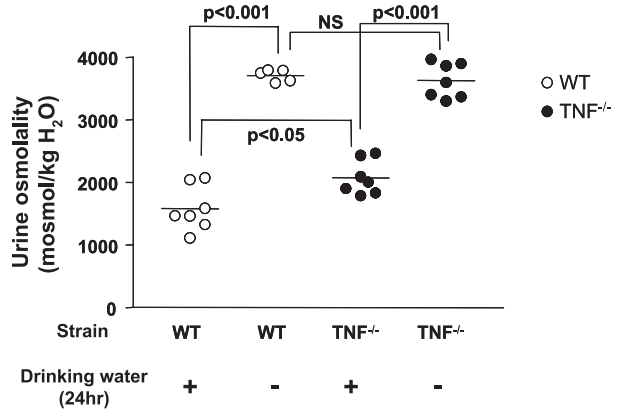

Fig. 4. Ambient osmolality and renal concentrating ability in WT and $TNF^{-/-}$ mice. Urine osmolality was measured in WT and $TNF^{-/-}$ mice before and after water deprivation for 24 h. Urine was collected and analyzed as described in MATERIALS AND METHODS.

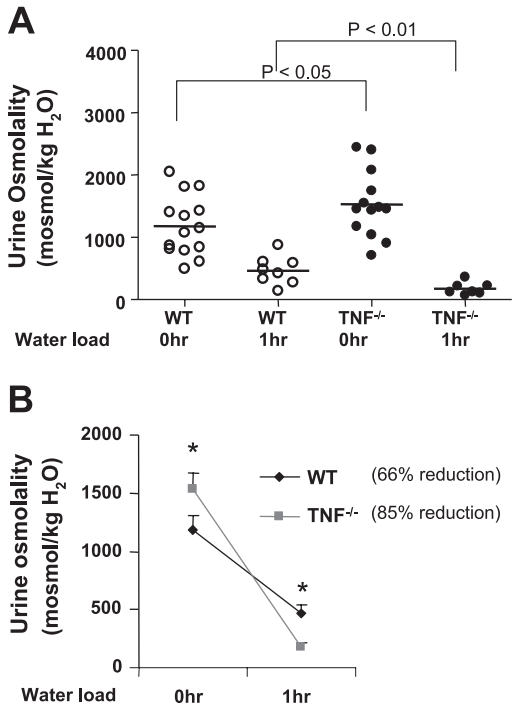

Fig. 5. Effects of water loading on urine osmolality in WT and TNF$^{-/-}$ mice. Mice were gavaged with water equivalent to 4% of their body weight. The urine collected before and after 1 h of water load was analyzed for osmolality. *A*: urine osmolalities determined before and after water loading of WT and TNF$^{-/-}$ mice. *B*: comparison of the percent change in urine osmolality before and after water loading. *$P < 0.05$ vs. urine osmolality at 0 h.

suggesting that TNF acts as an endogenous inhibitor of NKCC2 via activation of TNFR1. A comparison of serum parameters between WT and TNF$^{-/-}$ mice was unremarkable. However, urine osmolality was greater in TNF$^{-/-}$ compared with WT mice, suggesting that TNF may be an important contributor to the maintenance of ambient osmolality via effects on NKCC2A expression and activity. Urinary diluting ability also was greater in TNF$^{-/-}$ mice. An elevated basal urine osmolality and enhanced diluting ability in TNF$^{-/-}$ mice are consistent with increased NKCC2-mediated sodium reabsorption in the TAL.

The essential role of NKCC2 in establishing the medullary interstitial gradient is evident in studies using NKCC2$^{-/-}$ mice, which exhibit a lower ambient urinary osmolality than their WT littermates (41). Treatment of NKCC2$^{-/-}$ mice with vasopressin did not increase urine osmolaility because of their impaired ability to establish an interstitial gradient. Urine osmolality also did not increase after water deprivation in NKCC2$^{-/-}$ mice (41). Three alternative splice variants of NKCC2, NKCC2A, NKCC2B, and NKCC2F, account for 20, 10, and 70%, respectively, of the total NKCC2 transcript abundance in mice (3). Previous studies in NKCC2A$^{-/-}$ and NKCC2B$^{-/-}$ mice revealed a slight decrease in the ambient urine osmolality compared with control mice. Urine osmolalities in both genotypes were significantly higher in response to water deprivation, although the concentrating ability of these mice was not significantly different from that of WT littermates (28, 29). This may be due to the activity of NKCC2F, and in the case of NKCC2A$^{-/-}$ mice an additional compensatory increase in the NKCC2B isoform (29), which is sufficient to maintain the osmotic gradient in the medullary interstitium. The selective elevation of NKCC2A mRNA accumulation in TNF$^{-/-}$ mice was accompanied by an increase in NKCC2 activity in mTAL tubules and an increase in ambient urine osmolality. These observations are consistent with the notion that genetic deletion of TNF led to an increased interstitial gradient generated by elevated NKCC2A expression and activity, which is found in the OM as well as renal cortex. However, maximal urine osmolalities achieved 24 h after water deprivation were similar in WT and TNF$^{-/-}$ mice. Thus, although NKCC2A has a higher affinity for Na^+, K^+, and Cl^- compared with NKCC2F, the latter is the most abundant isoform and is present mainly in the inner stripe of the OM. The interstitial osmotic gradient increases axially through the medulla to the papillary tip and creates the driving force for vasopressin-elicited water reabsorption. Accordingly, the inability to detect differences in the maximal urine concentrating ability of WT and TNF$^{-/-}$ mice may reflect enhanced high-capacity transport mediated by NKCC2F. In response to water deprivation, vasopressin increases phosphorylation of NKCC2 in the mTAL, where the NKCC2F isoform is abundant. Since WT and TNF$^{-/-}$ mice have similar levels of NKCC2F, the ability to maximally concentrate urine is not different between these genotypes. Interestingly, urinary diluting ability was greater in TNF$^{-/-}$ compared with WT mice. The cortical TAL (cTAL) has a higher capacity for urine dilution compared with the mTAL (36, 37). This coincides with the presence of NKCC2A and NKCC2B isoforms in the cTAL, as previously described (18, 28), and suggests that elevation in NKCC2A in TNF$^{-/-}$ mice contributes to the greater diluting capacity observed in these mice.

The effects of TNF are mediated through two distinct TNF receptors, type 1 55-kDa TNFR (TNFR1) and type 2 75-kDa TNFR (TNFR2), which belong to the TNF receptor superfamily and are coexpressed on the surface of most cell types (42, 43). No information is available regarding TNF receptor expression in the mTAL, although mRNA for TNFR1 and TNFR2 are present in renal OM (Ferreri laboratory, unpublished observation). Since hTNF binds only to mouse TNFR1 (1), the inhibition of NKCC2A protein expression, mRNA accumulation, and activity in TNF$^{-/-}$ mice treated with hTNF most likely required activation of TNFR1-dependent signaling pathways. This interpretation is consistent with previous findings showing that the defect in renal concentrating ability in ARF is due to downregulation of various renal transporters, including NKCC2 (38), and that mice deficient in TNFR1 are resistant to endotoxin-induced ARF (7). Thus, while TNF is a mediator of renal inflammation in several models of hypertension as well as ARF, it also acts as a modulator of blood pressure regulation via interactions with molecules that regulate vascular and renal function. For instance, TNF may also contribute to the NO-dependent inhibition of electrolyte transport in the kidney (20, 31, 35). The extent to which systemic alterations in circulating hormones, changes in sympathetic nerve activity, or additional extrarenal mechanisms contribute to the present findings remains to be determined. However, acute administration of hTNF to anesthetized mice increased fractional excretion of sodium without affecting arterial pressure, illustrating dual functions of TNF mediated via TNFR1 activation acting as a renal vasoconstrictor and an inhibitor of renal tubular transport (39). The latter effect is consistent with

our laboratory's previous studies, demonstrating production of TNF by mTAL cells and a mechanism involving COX-2 that inhibits Na^+ transport in these cells, and supports the notion that TNF exerts direct effects on TAL tubules (10, 12). Other laboratories have demonstrated natriuretic and blood pressure-lowering effects of TNF (11, 27). Moreover, sublethal doses of TNF administered to dogs caused a marked polyuria and natriuresis (46). In the present study, the absence of TNF was associated with functional and molecular biological effects consistent with enhanced reabsorption in the TAL.

NKCC2 is subject to both short- and long-term regulation (8, 15). For instance, short-term regulation that is cAMP dependent affects trafficking to the apical membrane of the TAL (2, 30), while activation of a cAMP-responsive element in the *Slc12A1* promoter is an example of long-term regulation (19). However, it is likely that other regulatory mechanisms exist to control the activity and expression of this essential renal transporter, as NKCC2 isoforms are strategically expressed along the mTAL, cTAL, and macula densa. Alternative splicing is a critically important process that greatly increases the diversity of genes. It occurs in 60% of human genes, is common among genes encoding renal transporters, and results in the formation of nonfunctional dominant-negative proteins, as well as functional isoforms that affect trafficking of isoforms, kinetic properties, and location of proteins (3, 14). We observed a selective increase in NKCC2A mRNA accumulation in OM from $TNF^{-/-}$ mice, as the abundance of NKCC2F and NKCC2B was comparable in WT and $TNF^{-/-}$ mice. NKCC2 isoforms are derived from a single *Slc12A1* gene, and administration of hTNF inhibited NKCC2A mRNA accumulation but had no effect on NKCC2F and NKCC2B. Therefore, TNF may be part of a repressor mechanism in the TAL that, via activation of TNFR1, limits NKCC2A mRNA accumulation by regulating alternative splicing or exerting a posttranscriptional effect on mRNA half-life. The precise mechanisms by which TNF exerts a tonic suppressive effect on NKCC2A remains to be determined, and it is intriguing to speculate that TNF also may affect either alternative splicing and/or posttranscriptional mechanisms that regulate the expression of other renal transporter genes. Interestingly, TNF exerts a direct effect on renin gene transcription via activation of NF-κB, which, by binding to the cAMP-responsive element of the renin promoter, inhibits the transcription (45). NKCC2 also contains an NF-κB recognition site in its promoter, suggesting the possible regulation of NKCC2 gene transcription by TNF (19).

Our laboratory previously showed that TNF is produced by mTAL cells under baseline conditions and is present in urine of WT mice (6, 26). We hypothesize that TNF plays a role as an endogenous inhibitor of NKCC2A, an effect that may be dependent on TNFR1 activation and contribute to the maintenance of ambient urinary osmolality, as well as the diluting capacity of the kidney. Moreover, as TNF inhibits renin gene expression and $TNF^{-/-}$ mice exhibit enhanced basal renin levels (44), the molecular interactions that govern enhanced NKCC2A activity, which decreases chloride delivery to the macula densa, could contribute to stimulation of renin release (28, 29). The consequences of eliminating the tonic suppressive effect of TNF on NKCC2A are currently being studied as a function of changes in dietary NaCl intake.

ACKNOWLEDGMENTS

The authors thank Dr. Lisa Satlin and Beth Zavilowitz, Mount Sinai School of Medicine, for determination of urine osmolality (P30 DK079307; The Pittsburgh Center for Kidney Research: Physiology Core).

GRANTS

This work was supported by NIH grant HL085439.

DISCLOSURES

No conflicts of interest, financial or otherwise, are declared by the author(s).

REFERENCES

1. **Ameloot P, Fiers W, DeBleser P, Ware CF, Vandenabeele P, Brouckaert P.** Identification of tumor necrosis factor (TNF) amino acids crucial for binding to the murine p75 receptor and construction of receptor-selective mutants. *J Biol Chem* 276: 37426–37430, 2001.

1a. **Bao HF, Zhang ZR, Liang YY, Ma JJ, Eaton DC, Ma HP.** Ceramide mediates inhibition of the renal epithelial sodium channel by tumor necrosis factor-alpha through protein kinase C. *Am J Physiol Renal Physiol* 293: F1178–F1186, 2007.

2. **Caceres PS, Ares GR, Ortiz PA.** cAMP stimulates apical exocytosis of the renal Na^+-K^+-$2Cl^-$ cotransporter NKCC2 in the thick ascending limb: role of protein kinase A. *J Biol Chem* 284: 24965–24971, 2009.

3. **Castrop H, Schnermann J.** Isoforms of renal Na-K-2Cl cotransporter NKCC2: expression and functional significance. *Am J Physiol Renal Physiol* 295: F859–F866, 2008.

4. **Caverzasio J, Rizzoli R, Dayer JM, Bonjour JP.** Interleukin-1 decreases renal sodium reabsorption: possible mechanism of endotoxin-induced natriuresis. *Am J Physiol Renal Fluid Electrolyte Physiol* 252: F943–F946, 1987.

5. **Chamberlin ME, Mandel LJ.** Substrate support of medullary thick ascending limb oxygen consumption. *Am J Physiol Renal Fluid Electrolyte Physiol* 251: F758–F763, 1986.

6. **Chen CC, Pedraza PL, Hao S, Stier CT, Ferreri NR.** TNFR1-deficient mice display altered blood pressure and renal responses to ANG II infusion. *Am J Physiol Renal Physiol* 299: F1141–F1150, 2010.

7. **Cunningham PN, Dyanov HM, Park P, Wang J, Newell KA, Quigg RJ.** Acute renal failure in endotoxemia is caused by TNF acting directly on TNF receptor-1 in kidney. *J Immunol* 168: 5817–5823, 2002.

8. **Ecelbarger CA, Kim GH, Terris J, Masilamani S, Mitchell C, Reyes I, Verbalis JG, Knepper MA.** Vasopressin-mediated regulation of epithelial sodium channel abundance in rat kidney. *Am J Physiol Renal Physiol* 279: F46–F53, 2000.

9. **Eng B, Mukhopadhyay S, Vio CP, Pedraza PL, Hao S, Battula S, Sehgal PB, McGiff JC, Ferreri NR.** Characterization of a long-term rat mTAL cell line. *Am J Physiol Renal Physiol* 293: F1413–F1422, 2007.

10. **Escalante BA, Ferreri NR, Dunn CE, McGiff JC.** Cytokines affect ion transport in primary cultured thick ascending limb of Henle's loop cells. *Am J Physiol Cell Physiol* 266: C1568–C1576, 1994.

11. **Evans DA, Jacobs DO, Revhaug A, Wilmore DW.** The effects of tumor necrosis factor and their selective inhibition by ibuprofen. *Ann Surg* 209: 312–321, 1989.

12. **Ferreri NR, An SJ, McGiff JC.** Cyclooxygenase-2 expression and function in the medullary thick ascending limb. *Am J Physiol Renal Physiol* 277: F360–F368, 1999.

13. **Ferreri NR, Escalante BA, Zhao Y, An SJ, McGiff JC.** Angiotensin II induces TNF production by the thick ascending limb: functional implications. *Am J Physiol Renal Physiol* 274: F148–F155, 1998.

14. **Gamba G.** Alternative splicing and diversity of renal transporters. *Am J Physiol Renal Physiol* 281: F781–F794, 2001.

15. **Gimenez I, Forbush B.** Short-term stimulation of the renal Na-K-Cl cotransporter (NKCC2) by vasopressin involves phosphorylation and membrane translocation of the protein. *J Biol Chem* 278: 26946–26951, 2003.

16. **Hao S, Zhao H, Darzynkiewicz Z, Battula S, Ferreri NR.** Differential regulation of NFAT5 by NKCC2 isoforms in medullary thick ascending limb (mTAL) cells. *Am J Physiol Renal Physiol* 300: F966–F975, 2011.

17. **Hao S, Zhao H, Darzynkiewicz Z, Battula S, Ferreri NR.** Expression and function of NFAT5 in medullary thick ascending limb (mTAL) cells. *Am J Physiol Renal Physiol* 296: F1494–F1503, 2009.

18. **Igarashi P, Vanden Heuvel GB, Payne JA, Forbush B 3rd.** Cloning, embryonic expression, and alternative splicing of a murine kidney-specific

Na-K-Cl cotransporter. *Am J Physiol Renal Fluid Electrolyte Physiol* 269: F405–F418, 1995.
19. **Igarashi P, Whyte DA, Li K, Nagami GT.** Cloning and kidney cell-specific activity of the promoter of the murine renal Na-K-C1 cotransporter gene. *J Biol Chem* 271: 9666–9674, 1996.
20. **Kone BC, Higham S.** Nitric oxide inhibits transcription of the Na^+-K^+-ATPase α_1-subunit gene in an MTAL cell line. *Am J Physiol Renal Physiol* 276: F614–F621, 1999.
22. **Kreydiyyeh SI, Markossian S.** Tumor necrosis factor alpha down-regulates the Na^+-K^+ ATPase and the Na^+-K^+2Cl^- cotransporter in the kidney cortex and medulla. *Cytokine* 33: 138–144, 2006.
23. **Kwon TH, Frokiaer J, Han JS, Knepper MA, Nielsen S.** Decreased abundance of major Na^+ transporters in kidneys of rats with ischemia-induced acute renal failure. *Am J Physiol Renal Physiol* 278: F925–F939, 2000.
24. **Livak KJ, Schmittgen TD.** Analysis of relative gene expression data using real-time quantitative PCR and the 2[-delta delta C(T)] method. *Methods* 25: 402–408, 2001.
25. **Ma T, Yang B, Gillespie A, Carlson EJ, Epstein CJ, Verkman AS.** Severely impaired urinary concentrating ability in transgenic mice lacking aquaporin-1 water channels. *J Biol Chem* 273: 4296–4299, 1998.
26. **Macica CM, Escalante BA, Conners MS, Ferreri NR.** TNF production by the medullary thick ascending limb of Henle's loop. *Kidney Int* 46: 113–121, 1994.
27. **Nakatsuji K, Kii Y, Fujitani B, Ito T.** General pharmacology of recombinant human tumor necrosis factor. 1st communication: effects on cardiovascular, gastrointestinal, renal and blood functions. *Arzneimittelforschung* 40: 218–225, 1990.
28. **Oppermann M, Mizel D, Huang G, Li C, Deng C, Theilig F, Bachmann S, Briggs J, Schnermann J, Castrop H.** Macula densa control of renin secretion and preglomerular resistance in mice with selective deletion of the B isoform of the Na,K,2Cl co-transporter. *J Am Soc Nephrol* 17: 2143–2152, 2006.
29. **Oppermann M, Mizel D, Kim SM, Chen L, Faulhaber-Walter R, Huang Y, Li C, Deng C, Briggs J, Schnermann J, Castrop H.** Renal function in mice with targeted disruption of the A isoform of the Na-K-2Cl co-transporter. *J Am Soc Nephrol* 18: 440–448, 2007.
30. **Ortiz PA.** cAMP increases surface expression of NKCC2 in rat thick ascending limbs: role of VAMP. *Am J Physiol Renal Physiol* 290: F608–F616, 2006.
31. **Ortiz PA, Garvin JL.** NO inhibits NaCl absorption by rat thick ascending limb through activation of cGMP-stimulated phosphodiesterase. *Hypertension* 37: 467–471, 2001.
32. **Overbergh L, Valckx D, Waer M, Mathieu C.** Quantification of murine cytokine mRNAs using real time quantitative reverse transcriptase PCR. *Cytokine* 11: 305–312, 1999.
33. **Payne JA, Forbush B 3rd.** Alternatively spliced isoforms of the putative renal Na-K-Cl cotransporter are differentially distributed within the rabbit kidney. *Proc Natl Acad Sci U S A* 91: 4544–4548, 1994.
34. **Pfaffl MW.** A new mathematical model for relative quantification in real-time RT-PCR. *Nucleic Acids Res* 29: e45, 2001.
35. **Plato CF, Stoos BA, Wang D, Garvin JL.** Endogenous nitric oxide inhibits chloride transport in the thick ascending limb. *Am J Physiol Renal Physiol* 276: F159–F163, 1999.
36. **Reeves WB, Dudley MA, Mehta P, Andreoli TE.** Diluting power of thick limbs of Henle. II. Bumetanide-sensitive $22Na^+$ influx in medullary vesicles. *Am J Physiol Renal Fluid Electrolyte Physiol* 255: F1138–F1144, 1988.
37. **Rocha AS, Kokko JP, Burg MB.** Sodium chloride and water transport in the medullary thick ascending limb of Henle: evidence for active chloride transport 1973. *J Am Soc Nephrol* 10: 1145–1156, 1999.
38. **Schmidt C, Hocherl K, Schweda F, Kurtz A, Bucher M.** Regulation of renal sodium transporters during severe inflammation. *J Am Soc Nephrol* 18: 1072–1083, 2007.
39. **Shahid M, Francis J, Majid DS.** Tumor necrosis factor-alpha induces renal vasoconstriction as well as natriuresis in mice. *Am J Physiol Renal Physiol* 295: F1836–F1844, 2008.
40. **Sriramula S, Haque M, Majid DS, Francis J.** Involvement of tumor necrosis factor-alpha in angiotensin II-mediated effects on salt appetite, hypertension, and cardiac hypertrophy. *Hypertension* 51: 1345–1351, 2008.
41. **Takahashi N, Chernavvsky DR, Gomez RA, Igarashi P, Gitelman HJ, Smithies O.** Uncompensated polyuria in a mouse model of Bartter's syndrome. *Proc Natl Acad Sci U S A* 97: 5434–5439, 2000.
42. **Tartaglia LA, Goeddel DV.** Two TNF receptors. *Immunol Today* 13: 151–153, 1992.
43. **Tartaglia LA, Weber RF, Figari IS, Reynolds C, Palladino MA Jr, Goeddel DV.** The two different receptors for tumor necrosis factor mediate distinct cellular responses. *Proc Natl Acad Sci U S A* 88: 9292–9296, 1991.
44. **Todorov V, Muller M, Schweda F, Kurtz A.** Tumor necrosis factor-alpha inhibits renin gene expression. *Am J Physiol Regul Integr Comp Physiol* 283: R1046–R1051, 2002.
45. **Todorov VT, Volkl S, Muller M, Bohla A, Klar J, Kunz-Schughart LA, Hehlgans T, Kurtz A.** Tumor necrosis factor-alpha activates NFkappaB to inhibit renin transcription by targeting cAMP-responsive element. *J Biol Chem* 279: 1458–1467, 2004.
46. **van Lanschot JJ, Mealy K, Jacobs DO, Evans DA, Wilmore DW.** Splenectomy attenuates the inappropriate diuresis associated with tumor necrosis factor administration. *Surg Gynecol Obstet* 172: 293–297, 1991.
47. **Varela M, Garvin JL.** Acute and chronic regulation of thick ascending limb endothelial nitric oxide synthase by statins. *J Am Soc Nephrol* 15: 269–275, 2004.
48. **Wang D, Pedraza PL, Abdullah HI, McGiff JC, Ferreri NR.** Calcium-sensing receptor-mediated TNF production in medullary thick ascending limb cells. *Am J Physiol Renal Physiol* 283: F963–F970, 2002.
49. **Zeidel ML, Brady HR, Kohan DE.** Interleukin-1 inhibition of Na^+-K^+-ATPase in inner medullary collecting duct cells: role of PGE2. *Am J Physiol Renal Fluid Electrolyte Physiol* 261: F1013–F1016, 1991.